THE BIOLOGICAL EFFECTS OF DAILY TREATMENT UNCERTAINTY IN DOMINANT INTRAPROSTATIC LESION SIMULTANEOUS INTEGRATED BOOST USING INTENSITY MODULATED PROTON THERAPY

A Thesis
Presented to
The Academic Faculty

by

John D. DeMoor

In Partial Fulfillment
of the Requirements for the Degree
Master of Science in Medical Physics in the
George W. Woodruff School of Mechanical Engineering

Georgia Institute of Technology

May 2021

THE BIOLOGICAL EFFECTS OF DAILY TREATMENT UNCERTAINTY IN DOMINANT INTRAPROSTATIC LESION SIMULTANEOUS INTEGRATED BOOST USING INTENSITY MODULATED PROTON THERAPY

Approved by:

Dr. Jun Zhou, Advisor
Department of Radiation Oncology
Emory University School of Medicine

Dr. Chris Wang
School of Mechanical Engineering
Georgia Institute of Technology

Dr. Eric Elder
Department of Radiation Oncology
Emory University School of Medicine

Date Approved: April 21, 2021

Dedicated to my fiancée, Whitney Phelps

ACKNOWLEDGEMENTS

I would first like to thank Dr. Zhou as the primary advisor of this project for the contribution of so much of his valuable time and expertise. Second, I would like to thank Dr. Wang and Dr. Elder for their additional support in the creation of this thesis, and for the essential knowledge they imparted to me through their outstanding didactic coursework. Third, I would like to thank my classmates, Clara Glassman, Duncan Bohannon, and William LePain for countless insightful conversations that contributed to my understanding of numerous topics in the field of medical physics. Lastly, I would like to thank my parents Mark and Cathy DeMoor for their encouragement and endless support in all my educational endeavors, and my fiancée Whitney Phelps for her love and companionship.

TABLE OF CONTENTS

LIST OF TABLES

LIST OF FIGURES

LIST OF ABBREVIATIONS

IMPT – Intensity Modulated Proton Therapy

TCP – Tumor Control Probability

NTCP – Normal Tissue Complication Probability

mpMRI – Multiparametric Magnetic Resonance Imaging

DIL – Dominant Intraprostatic Lesion

SIB – Simultaneous Integrated Boost

CBCT – Cone Beam Computed Tomography

PTV – Planning Target Volume

CTV – Clinical Target Volume

ADC – Apparent Diffusion Coefficient

ROI – Region of Interest

LKB – Lyman-Kutcher-Burman

IMRT – Intensity Modulated Radiation Therapy

VMAT – Volumetric Modulated Arc Therapy

SBRT – Stereotactic Body Radiation Therapy

OAR – Organ at risk

SUMMARY

Intensity modulated proton therapy (IMPT) is a radiation therapy treatment modality that offers superior dose conformity in the treatment of a variety of cancers. IMPT may deliver simultaneous integrated boost (SIB) to dominant intraprostatic lesions (DILs) detected by multiparametric MRI (mpMRI) to improve tumor control in prostate patients. DIL-SIB delivered using traditional photon therapy techniques has been demonstrated to achieve better clinical outcomes. IMPT can deliver a larger dose to the DIL than photons but is more susceptible to dosimetric variation from interfractional anatomic changes. The purpose of this thesis is to evaluate the efficacy of IMPT DIL-SIB plans and their sensitivity to daily anatomy changes through calculation of tumor control probability (TCP) and normal tissue complication probability (NTCP).

CHAPTER 1. INTRODUCTION

1.1 Motivation

The purpose of radiation therapy in oncology is to control or eradicate cancer cells without causing unacceptable damage to normal tissues. Therefore, the goal of any treatment plan with a given modality is to maximize the dose delivered to the delineated tumor volume while minimizing the dose to organs at risk (OARs). More specifically, a plan must deliver a minimum prescribed dose to a certain percentage of the target without exceeding maximum dose constraints for normal tissues. The question of which radiation therapy modalities and techniques provide the best results for a given tumor type has been the subject of extensive research. Proton beam therapy is a unique modality that has been applied in the treatment of many different cancers. The characteristic dose distribution of protons, in which a significant portion of the energy is deposited at the end of each particle track, can be leveraged to decrease dose to normal tissues. Modern treatment delivery techniques such as pencil beam scanning may be used to deliver intensity modulated proton therapy (IMPT), in which the dose rate is modulated throughout the treatment to ensure conformity. Controversy exists over whether the additional cost of proton therapy is justified by clearly superior patient outcomes. Long-term clinical studies on the benefits of proton therapy are still forthcoming for many cancers, with early evidence often conflicting. New treatment techniques that maximize the advantages of proton therapy over traditional radiation therapy modalities could justify its use, even at a much higher cost. The safety and effectiveness of any new treatment technique may be supported through

dosimetric and biological analysis of planning data in the absence of clinical trials investigating actual patient outcomes.

1.2 Proton Therapy for Prostate Cancer

Prostate carcinoma is the most common cancer occurring in men within the United States, accounting for twenty-one percent of new malignances in 2020. It is also responsible for ten percent of male cancer deaths, second only to lung and bronchus cancers. Despite its commonality, widespread screening and a multitude of treatment techniques have made the survival rate high (1). Radiation therapy has been widely used in the treatment of prostate cancer for decades. Different modalities and techniques including intensity modulated radiation therapy (IMRT), volumetric modulated arc therapy (VMAT), stereotactic body radiation therapy (SBRT) and interstitial brachytherapy are prescribed depending on the cancer stage and preferences of the patient. The benefits of these treatment options in patients of different ages and cancer stages have been the topic of many clinical studies and literature. Proton beam therapy has been employed in prostate cancer treatment since the early 1990s. Widespread information reporting the theoretical benefits of protons has led an increasing number of patients to pursue this type of treatment. Prostate patients now account for the majority of proton therapy procedures performed in the United States. As previously mentioned, the superior dose conformity that may be achieved through the interaction characteristics of protons can decrease the likelihood of normal tissue toxicities without sacrificing tumor control. Long-term clinical studies demonstrating the benefits of proton therapy for prostate cancer are lacking, as with other cancers (2). Initial studies of clinical outcomes have compared proton therapy to other modalities using criteria such as tumor control, gastrointestinal and genitourinary

toxicities, as well as the risk of secondary malignancies. The results of these studies are widely mixed (3).

1.3 New Treatment Methods

New techniques for the planning and delivery of proton therapy offer the opportunity to increase its efficacy and advantages in the treatment of prostate cancer. Modern IMPT delivered using pencil beam scanning is superior to traditional passive scattering when considering both range and dose precision (4). IMPT may also be used to accurately deliver additional radiation dose to tumor lesions within the prostate, instead of the usual homogenous irradiation of the whole volume. This technique may increase the probability of tumor control, while also increasing the occurrence of normal tissue damage. A significant issue with even modern proton therapy techniques is dosimetric uncertainty, the effects of which are made worse by the larger dose deposited over a narrower range. Setup errors, range variation, and anatomy changes between fractions can significantly alter the planned dose distribution in prostate patients (5) (6). Dose escalation can increase the potential for unplanned dose shifts to cause normal tissue damage, as the focal spots covering the lesions deliver a very high dose. For novel treatment methods such as IMPT prostate lesion boost to be promoted for clinical use, their safety and effectiveness must be demonstrated. The analysis of biological endpoints presented in this thesis will provide a basis for the use of lesion boost over conventional plans in IMPT, and possibly support the superiority of proton therapy in the treatment of prostate cancer through this technique.

CHAPTER 2. BACKGROUND

2.1 Prostate Patient Simulation

Simulation methods used in radiation therapy treatment planning for prostate patients typically include CT and MRI registrations that are used to identify the prostate, OARs and bony anatomy. Other tools such as fiducial markers and dyes may also be implemented to localize the target and significant organs. A unique MR imaging technique, known as multiparametric MRI (mpMRI) has recently been incorporated into the screening, diagnosis, and simulation of prostate cancer. MpMRI typically combines T1, T2 and diffusion weighted scans to increase soft tissue contrast and conspicuity. These images may be used to detect tumor lesions within the prostate and identify the region of greatest disease prominence, known as the dominant intraprostatic lesion (DIL) (7). The ability to identify the DIL in prostate patients presents the opportunity for more targeted treatment options, the most significant being radiotherapy boost.

2.2 DIL-SIB

Once the mpMRI-defined DIL is identified in a prostate patient, a focal boost of radiation dose may be delivered to the lesion. The feasibility of DIL focal boost in the treatment of prostate cancer has been demonstrated using several different modalities. In patients undergoing interstitial brachytherapy, optimized needle patterns may be used to deliver additional dose to the DIL for better tumor control (8). A common technique for the delivery of focal dose boost using external beam modalities is simultaneous integrated boost (SIB), in which varying dose levels are delivered to different target volumes in the

same treatment fraction (9). Clinical studies have demonstrated that DIL-SIB is safe and effective when delivered with photon IMRT and VMAT. These studies, when comparing DIL-SIB with conventional plans, show an improvement in tumor control and disease-free patient survival without a significant increase in normal tissue toxicities (10) (11). DIL-SIB may be administered with IMPT using pencil-beam scanning, in which a number of small beamlets are delivered to the target one energy layer at a time. During treatment planning, the target volumes are covered with beam spots to deliver a certain dose level to the tumor. Evidence supporting the feasibility and possible superiority of DIL-SIB using IMPT is much less established, but compelling. Due to the greater dose conformity of protons, DIL-SIB delivered with IMPT has been demonstrated to achieve a higher dose to the DIL when compared with IMRT or VMAT without violating OAR constraints (12). Other planning studies also suggest that IMPT DIL-SIB may improve tumor control while meeting all required normal tissue objectives (13).

2.3 Dosimetric Uncertainty

A significant problem in modern proton therapy is uncertainty between the planned and delivered dose distributions. Any errors or variation in the delivery of a treatment plan may have more significant dosimetric consequences than in photon therapy. This is due to the characteristic dose distribution of protons, where a larger amount of the dose is deposed over a smaller range. In a typical proton therapy treatment plan, the edges of the Bragg peak are aligned with the target volume. Since the dose falloff beyond the Bragg peak is abrupt, errors during delivery may result in a higher overdose to tissues outside the target volume and loss of proper target coverage. One possible source of error is uncertainty in the tissue proton ranges calculated during the treatment planning phase. In photon therapy,

linear attenuation coefficients of various tissues correlate very closely with Hounsfield units calculated from CT simulation. Proton stopping powers, however, cannot be estimated with the same accuracy from CT. This leads to a residual uncertainty in the range of proton beams and a greater influence of tissue heterogeneity on the dose distribution. Therefore, a hallmark of a good proton treatment plan is low susceptibility to possible uncertainties in the range, known as robustness. Plans may be optimized based on robustness objectives to ensure that the clinical goals are preserved in the presence of range variation. A typical standard for acceptable robustness is ±3.5% deviation in the planned ranges, as this is the usual uncertainty associated with the proton stopping powers calculated from CT scans. A common way that range uncertainties are accounted for in a treatment plan is by adding a margin to the delineated clinical target volume (CTV) to create the planning target volume (PTV) (14). Additional errors that may alter the delivered dose distribution include inaccurate patient setup, as well as changes in patient anatomy both during and between treatment fractions. In prostate patients, anatomic changes resulting in dosimetric variation can include femur rotation, adipose tissue thickness, and rectal and bladder filling (5) (6). Techniques for minimizing this variation include patient immobilization deceives, marking and mapping systems for alignment, margins to account for motion, and rectal and bladder filling protocols. Some movement is inevitable even when using these techniques, although the extent of the dosimetric variation may not be predictable. Delivery of focal dose boost to DILs can increase the consequences of any variation in positioning or anatomy throughout the treatment. Doses delivered to the DIL with SIB may be as high as twice that of the typical uniform dose prescribed to the prostate volume. Imprecise delivery of the boost to the DIL can therefore result in significant

overdosing of normal tissues in the vicinity of the prostate, rendering the plan unsafe. Establishing the safety of IMPT DIL-SIB plans against large dosimetric variation would significantly support the practicality of their clinical use.

2.4 Tumor Control and Normal Tissue Toxicity

A variety of normal tissue toxicities may occur in the pelvic region as the result of overdosing from prostate radiotherapy. Extensive literature exists on different endpoints, both early and late, occurring in OARs if certain dose-volume thresholds are exceeded during treatment. Major OARs in the pelvic region include the rectum, bladder, bowel, urethra, bony anatomy, and sexual organs (15). Rectal toxicities are the most common and widely studied complications associated with prostate radiotherapy. The most frequent symptom of overdose to the rectum is bleeding, although other early and late effects may include necrosis/stenosis, incontinence, and diarrhea (16). Possible injuries to the bladder include urinary symptoms, contracture, and necrosis (17). Although less common, effects on the pelvic bony anatomy may involve necrosis and increased fracture risk of the femoral heads and pelvis (15). Overdose of the urethra may result in perforation and stricture followed by corresponding urinary symptoms (18). Bowel overdose may result in similar symptoms as rectal toxicity, such as diarrhea and incontinence (15). Sexual dysfunction may be caused by overdose of the penile bulb, testicles, and neurovascular bundles (15). During treatment planning, normal tissue toxicities may be avoided by ensuring that recommended dose-volume thresholds for certain tissues are not exceeded. Tissues with serial structure will have a higher threshold dose at a lower volume percentage, as overdose to even a small portion can cause serious damage to the function of the organ. Tissues with parallel structure typically have a higher threshold volume that may be irradiated to a lower

threshold dose (19). Treatment plans may be optimized based on normal tissue objectives to ensure that the planning doses do not exceed the recommended thresholds. Optimization based on tumor coverage is also necessary so that meeting normal tissue requirements does not compromise the dose prescribed to a given percentage of the tumor volume. One way of evaluating a treatment plan in terms of tumor control and normal tissue sparing is through tumor control probability (TCP) and normal tissue complication probability (NTCP). These values may be calculated by combining dose-response and statistical models to assess the probability of eradicating all tumor cells in the target volume or inducing a given complication in a normal tissue. While more traditional TCP and NTCP models are based on dose-volume histograms, modern methods may calculate dose response on the voxel level. This allows the model to consider irradiation of different tissues from a non-uniform dose distribution (20). Although not accurate representations of actual probabilities, TCP and NTCP are extremely useful for comparison of different treatment plans and evaluation of the effects of dosimetric changes (21). Calculations of these biological metrics for IMPT DIL-SIB plans may establish their benefits in terms of tumor control, evaluate the detriment to normal tissues, and assess how dosimetric variation from interfractional anatomy changes affects the plan.

CHAPTER 3. METHODS

3.1 Patient Data and Simulation

The data used for this study was obtained from twenty-five prostate patients previously treated at Emory Proton Therapy Center in early 2019. RayStation 8B served as the primary framework for simulation, planning, and biological evaluation. Prior to their treatment, each of the patients were scanned with a CT simulator. MR scans with T1, T2 and diffusion weighting were then acquired on the same day using an identical patient setup. The obtained MR images were compiled into apparent diffusion coefficient (ADC) maps. The resulting mpMR images were then rigidly registered with the CT scans to form the main planning images. These images were used to identify and contour the prostate and DIL for each patient. The CTV was created based on the contour of the prostate, and an additional margin added for the PTV to account for range and setup uncertainties. Significant OARs including the bladder, rectum, femoral heads, and urethra were also contoured. A series of pre-treatment cone beam CT (CBCT) scans were acquired for each patient over the first several days of treatment to assess the anatomy changes between fractions. Most patients received four to five scans during the first week of treatment, although several received more scans over a longer period. An important assumption made is that the anatomy changes occurring during this time frame are mostly representative of the entire treatment course, which lasted over a month. Several techniques were implemented during treatment and simulation to help reduce setup errors and motion. Fiducial markers were implanted into the prostate of each patient to assist with target localization and alignment for each treatment fraction. Patients were also secured with vacuum cushions during simulation and

treatment and asked to follow protocols of drinking 500 mL of water one hour before treatment and having an empty rectum for all procedures.

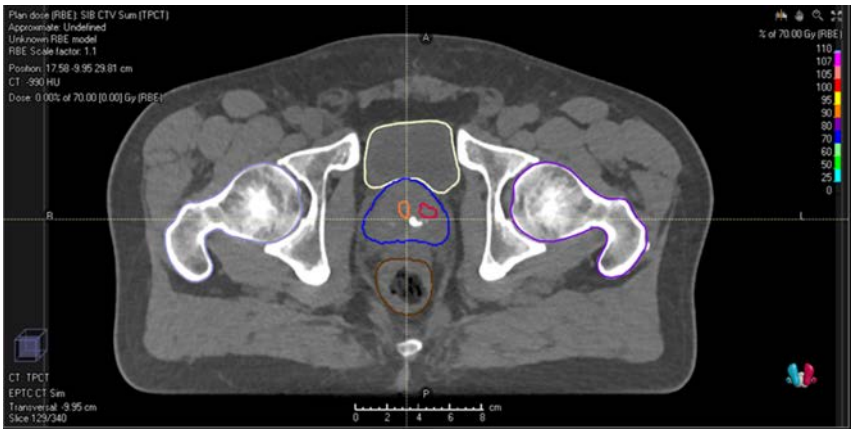

Figure 1 – Planning image showing contours of the DIL, prostate CTV and OARs

3.2 Treatment Planning

Two main treatment plans were created in RayStation for each of the twenty-five patients using the planning CT and mpMR registered images. Conventional clinical plans delivering the traditional uniform dose to the prostate were designated as “Prostate CTV”. These plans were created to deliver a dose of 70 Gy to 98% of the prostate CTV volume in 28 treatment fractions, using two lateral opposed beams. The DIL-SIB plans were then created to achieve the original uniform coverage of the prostate CTV, with an additional coverage of 98 Gy to > 95% of the contoured DIL volume. The original beam configuration was used for the SIB plans, with the pencil beam spot weighting at different energy levels optimized to achieve the objectives. The dose in the SIB plans was prescribed in the same number of treatment fractions as in the conventional plans. The completed SIB plans were designated as “SIB CTV”. Both the conventional and SIB plans were optimized based on

the prescribed target coverages, in addition to robustness and normal tissue objectives. Robust optimization accounted for 5 mm setup uncertainties in all directions and ±3.5% uncertainty in proton range. The maximum dose objectives used for normal tissues included bladder < 71.5 Gy, rectum < 71 Gy, femoral head < 40 Gy and urethra < 82 Gy. An additional dose falloff objective was also added to the DIL in the SIB plans to prevent excessive dose to the CTV. To incorporate the dosimetric variation from interfractional anatomy changes, separate composite plans were constructed using the series of daily CBCT scans. Anatomic changes reflected by the scans were integrated into the patient simulation model by deforming the initial planning CT images onto the daily scans, which had been registered to the fiducial markers before each treatment. The original contours of the CTV, DIL, urethra and femoral heads were copied to these deform registrations, while the rectum and bladder were redrawn based on the CBCT. The nominal treatment plans, both conventional and SIB, were then applied to the deformed images and the planning doses recalculated. To achieve the same effective dose as the nominal plans, the new daily planning doses calculated on the deformed planning CTs were summed into single plans. Each daily dose was multiplied by a certain factor required to achieve the same number of treatment fractions as the original plans. The two composites made for the conventional and SIB plans were designated as “Prostate CTV Sum” and “SIB CTV Sum”, respectively.

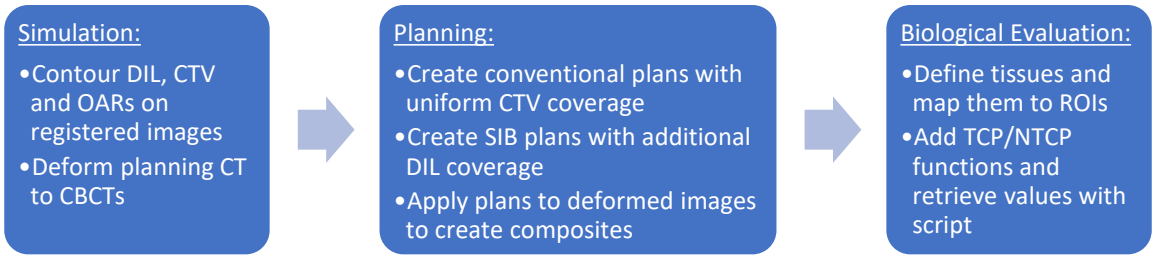

Figure 2 – Workflow steps of the project methodology

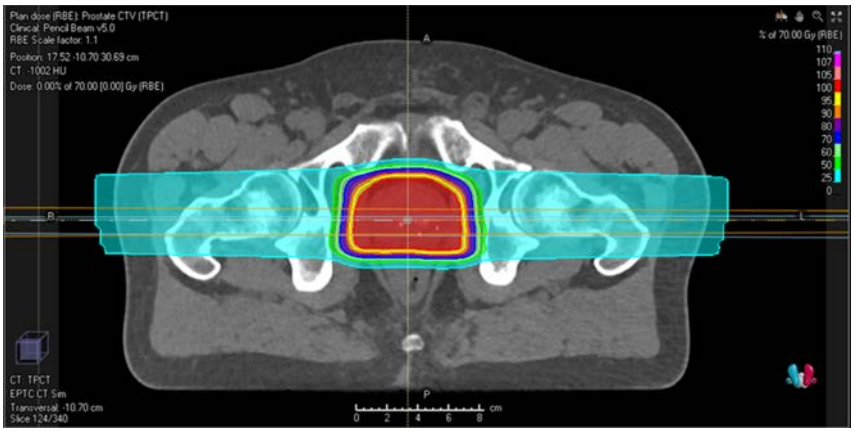

Figure 3 – Uniform dose distribution of conventional clinical plan

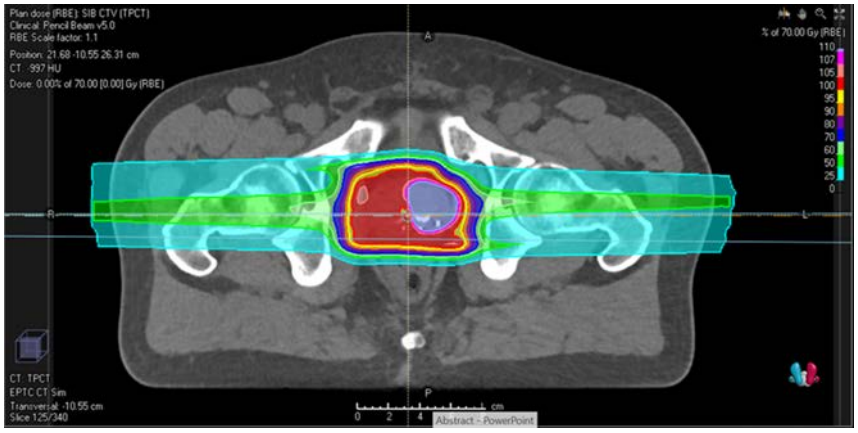

Figure 4 – Non-uniform dose distribution of DIL-SIB plan

3.4 Biological Evaluation

All calculations of TCP and NTCP for the four treatment plans were performed in the RayBiology module of RayStation 8B. This program contains different models and tools for evaluating the biological response of tissues to the doses from a given treatment plan. Individual tissues may be defined in terms of their various radiobiological parameters, then mapped to a particular region of interest (ROI) in the patient simulation. The dose response

of the ROI may then be modelled in terms of either tumor control or normal tissue complications. A series of functions for various targets and normal tissues may be added during treatment plan evaluation and used to compare different fractionation schedules or dose distributions. All models are voxel-based, first calculating and then summing the responses of each voxel in a given ROI. It is assumed that the tissues of tumors and organs modeled are relatively homogenous in structure. Most of the data for this study was processed with Python scripts in the RayStation scripting interface. This includes mapping ROIs with their given tissues, adding biological functions, and calculating the results.

3.5 TCP Modelling

TCP was defined in the background section as the probability of eradicating all clonogenic cells in a tumor volume. As tumors are generally considered to be parallel in tissue organization, even a small number of remaining cells can repopulate the tumor and cause relapse. TCP is commonly calculated through a combination of the linear-quadratic cell survival model and Poisson statistics. The most basic equation may be expressed in terms of both theoretical and clinical parameters as follows (22).

$$P(D) = e^{-N_0 e^{-\alpha n d - \beta n d^2}} = e^{-e^{e\gamma - \left(\frac{nd}{D_{50}}\right)(e\gamma - ln ln 2)}} \quad (1)$$

Where *P(D)* is the response probability from a given dose distribution, N_0 is the initial number of clonogenic tumor cells, *d* is the fractional dose, *n* is the number of treatment fractions, α and β are the linear quadratic fractionation parameters, γ is the maximum slope of the dose-response curve, and D_{50} is the dose to achieve a fifty percent response probability. The equation assumes that these parameters were derived from clinical trials in which a fixed fractionated dose was used (22). As a means of accounting for different

fractionation schedules, the total dose *nd* may be represented as the equivalent dose delivered in fractions of 2 Gy. This quantity, EQD_2, can be expressed as follows (23).

$$EQD_2 = \frac{nd\left(1+\frac{d}{\alpha/\beta}\right)}{1+\frac{2}{\alpha/\beta}} \tag{2}$$

Where all parameters are the same as in equation (1). A more general formula for calculating the EQD_2 from unequal fractional doses delivered to different partial volume elements is the following (23).

$$EQD_{2,i} = \frac{\sum_{k=1}^{n}\left\{d_{k,i}\left(1+\frac{d_{k,i}}{\alpha/\beta}\right)\right\}}{1+\frac{2}{\alpha/\beta}} \tag{3}$$

Where $EQD_{2,i}$ is the EQD_2 of a volume element or voxel, i is the voxel number, k is the fraction number, and $d_{k,i}$ is the dose to voxel i from fraction k. By combining equations (1) and (3), the Poisson-LQ TCP model used in the RayBiology module may be expressed in both the theoretical and clinical forms as follows (23).

$$TCP(D) = \prod_{i=1}^{M}\left[exp\left(-N_0 exp\left(\sum_{k=1}^{n}\left\{-\alpha d_{k,i} - \beta d_{k.i}^2\right\}\right)\right)\right]^{\frac{v_i}{v_{ref}}}$$

$$= \prod_{i=1}^{N_v}\left[exp\left(-exp\left[e\gamma - \frac{EQD_{2,i}}{D_{50}}(e\gamma - \ln(\ln(2)))\right]\right)\right]^{v_i/v_{ref}} \tag{4}$$

Where v_i is the volume of a voxel, v_{ref} is the total reference volume, M is the total number of voxels, and N_v is the total number of EQD_2 from all voxels. These equations account for non-uniform dose distributions by calculating the response of a partial volume, and then summing the responses from all partial volumes in the ROI. This model was used in the study to calculate the TCP for two target volumes in each plan, the contoured DIL and the prostate CTV minus the DIL. The choice was made to calculate TCP for these volumes

separately due to differing model parameters between the prostate and lesion tissues (24) (25). Similar methodology has also been used in other studies where TCP was calculated for prostate lesions (8). The parameters for the Poisson-LQ model used in this study are summarized in Table 1. The values of D_{50} and γ for the prostate and DIL were obtained from a study in which clinical patient follow-up data was fitted to the Poisson-LQ model (25). Since the α/β parameter for prostate cancer has still not been estimated precisely (26), the TCP calculations were performed twice using the two common values of 1.5 and 3.0. These represent reasonable higher and lower estimates of the actual value and have been used in similar studies (8). The TCP values for multiple tumors treated by the same plan may be combined through simple multiplication into a single value. The composite TCP, which expresses the total probability of controlling all tumor sites, can be calculated by the following equation (23).

$$TCP(D) = \prod_j TCP_j(D) \quad (5)$$

Where $TCP_j(D)$ is the TCP from dose D of target volume j.

Table 1 – Parameters used for the Poisson-LQ TCP model

Target	α/β (Gy)	D_{50} (Gy)	γ	Reference
DIL	1.5 / 3.0	68.1	4.5	(25)
Prostate CTV	1.5 / 3.0	66.8	3.8	(25)

3.6 NTCP Modelling

The RayBiology module contains two different models for estimating NTCP. The first is based on a similar combination of the linear-quadric response model and Poisson statistics as the TCP model. The primary difference is that the normal tissues considered by any NTCP model are partially serial in nature, instead of entirely parallel as with tumors. This structural difference leads to a unique volume dependence in normal tissues, which may be accounted for by an additional parameter. The relative seriality NTCP model incorporates the parameter *s*, which represents the fraction of total functional subunits in the tissue volume that are serial in nature (27). A small value of the *s* parameter therefore implies a minimal sensitivity to dose hot spots. Based on the relative seriality model, the RayStation equation for the Poisson-LQ NTCP model may be expressed as follows (23).

$$NTCP_{P-LQ}(D) = \left(1 - \prod_{i=1}^{M}\left(1 - \left[exp\left(-N_0 exp\left(\sum_{k=1}^{n}\{-\alpha d_{k,i} - \beta d_{k.i}^2\}\right)\right)\right]^{s}\right)^{\frac{v_i}{V_{ref}}}\right)^{\frac{1}{s}}$$

$$= \left(1 - \prod_{i=1}^{M}\left(1 - \left[exp\left(-exp\left[e\gamma - \frac{EQD_{2,i}}{D_{50}}(e\gamma - \ln(\ln(2)))\right]\right)\right]^{s}\right)^{v_i/V_{ref}}\right)^{1/s} \quad (6)$$

Where *s* is as defined above, and all other parameters are the same as in equation (4). The second NTCP model included in the RayBiology module is based on significantly different principles than either Poisson-LQ model. The Lyman-Kutcher-Burman (LKB) NTCP model uses an integral to calculate the total response probability of a number of partial volumes using estimations from known responses. The RayStation formulation of the model includes the three following separate equations (23).

$$NTCP_{LKB}(D) = \frac{1}{2\pi}\int_{-\infty}^{t} exp\left(\frac{-u^2}{2}\right) du \quad (7)$$

$$t = \frac{D_{eff} - D_{50}}{m \cdot D_{50}} \quad (8)$$

$$D_{eff} = \sum_{i=1}^{M} \left(\frac{v_i}{V_{ref}} EQD_{2,i}^{1/n} \right)^n \quad (9)$$

Where t is the standard deviation of the dose-volume distribution, D_{eff} is the equivalent uniform dose, m is the slope of the response curve, and n is the volume dependence of the tissue. The first equation expresses the NTCP as an integral based on a probit function, the second calculates the standard deviation, and the third converts the partial volume doses into the equivalent uniform dose (23) (28). The relative seriality model was favored for this study, as it has a more robust biological base and accounts for the seriality of tissues. The LKB model, however, has a much longer history of clinical use and more extensive literature estimating its parameters. Based on the availability of reliable model parameters for desired organs and endpoints, the relative seriality model was used to calculate NTCP for the bladder and femoral heads, while the LKB model was used for the urethra and rectum. These OARs and their given endpoints were chosen to represent common normal tissue toxicities prevalent in prostate patients, and for their use in other similar studies (29). The parameters used with a given model for each OAR and its corresponding endpoints are summarized in Table 2. NTCP values calculated for different OARs in the same treatment plan may also be combined into a single composite value. The composite NTCP considering j OARs may be calculated using the following formula (23).

$$NTCP(D) = 1 - \prod_j (1 - NTCP_j(D)) \quad (10)$$

Where $NTCP_j(D)$ is the *NTCP* from dose *D* of normal tissue *j*. The composite TCP and NTCP values for a given plan can be used to calculate the following single metric to assess the overall quality of the plan (23).

$$P_+ = TCP(D)(1 - NTCP(D)) \quad (11)$$

Where P_+ is the probability of complication-free tumor control, *TCP(D)* is the composite TCP and *NTCP(D)* is the composite NTCP. If composite NTCP and P_+ values were being used as an objective measurement of individual plan quality, the OARs considered would have to be carefully chosen. Minor complication endpoints that have the same NTCP as serious toxicities could not be given the same weight for obvious reasons. Since these metrics are only being used to compare plans in this study, all OARs for which NTCP was calculated will be considered.

Table 2 – Parameters used for the relative seriality and LKB NTCP models

OAR	Endpoint	α/β (Gy)	D_{50} (Gy)	γ	s	n	m	Reference
Rectum	≥ Grade 2 Bleeding	3.0	76.9	-	-	0.09	0.13	(16)
Femoral Heads	Necrosis	3.0	65.0	2.7	1.0	-	-	(30)
Bladder	Contracture	3.0	80.0	3.0	0.18	-	-	(30)
Urethra	Stricture	3.0	116.7	-	-	0.3	0.23	(18)

CHAPTER 4. RESULTS

4.1 Dosimetric and Anatomic Variation

Several measurements were made before the biological evaluation to assess the daily variations in patient anatomy and the resulting changes in the dosimetry of the plans. Average anatomic changes shown by the daily CBCT scans include a 0.6% increase in bladder volume, a 12.8% increase in rectal volume, and a 3.16 mm shift in femur position. Average dosimetric variations in the SIB plans include a 1.1% decrease in the CTV D99, a 3.1% decrease in the DIL V98, a 3.6% increase in the max bladder dose, and a 6.8% increase in the max rectum dose. These measurements give some context to the TCP and NTCP results and how they are affected by the dosimetric variation (31).

4.2 TCP Data

With the TCP computed for both the CTV and DIL using the two different α/β ratios, a total of four TCP values were collected for each plan. Sixteen were therefore recorded for each patient from the four created plans. The composite TCP was calculated by multiplying the individual TCPs of the CTV and DIL, for both α/β ratios. The mean values of each TCP obtained from all twenty-five patients are summarized in Table 3. The plots (a) and (b) in Figure 5 show the distribution of composite TCP data for both α/β values.

Table 3 – Mean TCP values for each plan

Plan	TCP DIL ($\alpha/\beta = 1.5$)	TCP CTV ($\alpha/\beta = 1.5$)	TCP DIL ($\alpha/\beta = 3$)	TCP CTV ($\alpha/\beta = 3$)	Comp. TCP ($\alpha/\beta = 1.5$)	Comp. TCP ($\alpha/\beta = 3$)
Prostate CTV	0.95309 ±0.00099	0.94217 ±0.00031	0.91508 ±0.00134	0.90452 ±0.00097	0.89798 ±0.00111	0.82773 ±0.00184
SIB CTV	0.99977 ±0.0002	0.95481 ±0.00129	0.99957 ±0.00033	0.92478 ±0.00203	0.95458 ±0.00131	0.92438 ±0.00205
Prostate CTV Sum	0.95166 ±0.00125	0.94132 ±0.00076	0.91272 ±0.00188	0.90307 ±0.00102	0.89584 ±0.00175	0.82428 ±0.00249
SIB CTV Sum	0.99992 ±0.00004	0.95508 ±0.0013	0.99978 ±0.0001	0.92521 ±0.00204	0.95500 ±0.0013	0.92501 ±0.00204

4.3 NTCP Data

As described in the methodology, the NTCP was evaluated in each plan for the urethra, rectum, bladder, and left and right femoral heads. The calculations from all four plans therefore include twenty NTCP values for each patient. The composite NTCP was calculated for each individual plan considering the NTCP for all OARs. The P+ values were also calculated using the composite NTCP and the composite TCP with both α/β ratios. The mean NTCP values for each OAR and the composite NTCPs are shown in Table 4. The mean P+ calculations for the two α/β rations are shown Table 5. The distribution of the composite NTCP data is shown by plot (c) in Figure 5.

Table 4 – Mean NTCP values for all OARs in each plan

Plan	NTCP Urethra	NTCP Rectum	NTCP Fem_H_L	NTCP Fem_H_R	NTCP Bladder	Composite NTCP
Prostate CTV	0.07762 ±0.00070	0.02440 ±0.00709	0±0	0±0	0.00006 ±0.00003	0.10016 ±0.00672
SIB CTV	0.08722 ±0.00197	0.02487 ±0.00789	0±0	0±0	0.00018 ±0.00009	0.11000 ±0.00778
Prostate CTV Sum	0.07718 ±0.00086	0.02280 ±0.00626	0±0	0±0	0.00004 ±0.00002	0.09823 ±0.00604
SIB CTV Sum	0.08939 ±0.00292	0.02680 ±0.00757	0±0	0±0	0.00014 ±0.00008	0.11379 ±0.00803

Table 5 – Mean P+ values for each plan using TCP from both α/β ratios

Plan	P+ ($\alpha/\beta = 1.5$)	P+ ($\alpha/\beta = 3.0$)
Prostate CTV	0.80807±0.00625	0.74486±0.00593
SIB CTV	0.84955±0.00739	0.82266±0.00725
Prostate CTV Sum	0.80779±0.00534	0.74325±0.00506
SIB CTV Sum	0.84634±0.00774	0.81976±0.00766

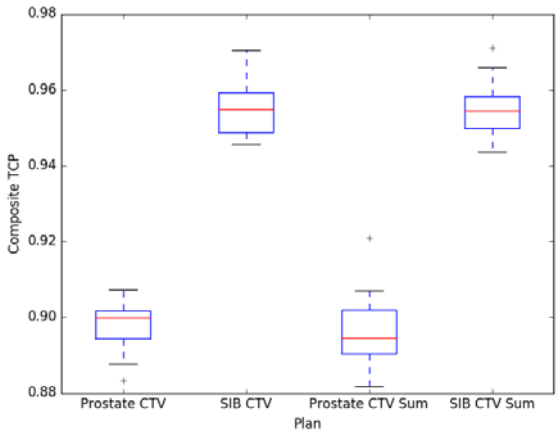

(a) Composite TCP (α/β = 1.5)

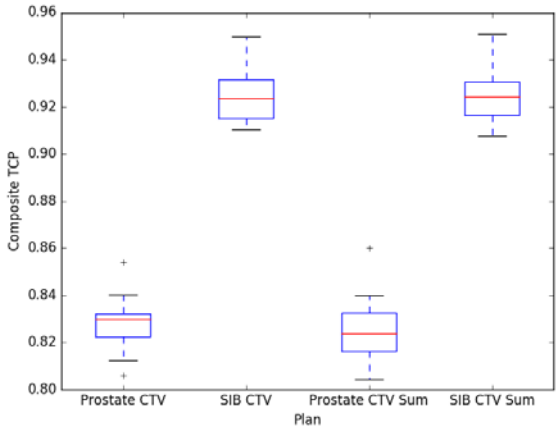

(b) Composite TCP (α/β = 3.0)

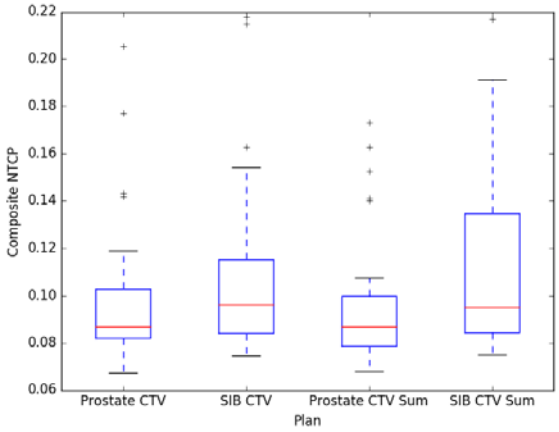

(c) Composite NTCP

Figure 5 – Distribution of composite TCP and NTCP data from all patients

4.4 Hypothesis Testing

The uncertainties assigned to each of the mean values listed in Tables 3-5 were calculated as the standard error of the sample mean, using the sample standard deviation. A series of hypothesis tests were performed with the mean values and standard deviations using a two-tailed pooled t-test for two normal means with variances approximately equal. The null hypothesis of these tests assumes no difference in the sample means being compared, with the alternative hypothesis being a significant difference. These tests were performed for the comparison of the mean composite TCPs and NTCPs between the conventional and SIB plans, and additionally between the nominal and composite forms of both plans. The p-values calculated from the hypothesis tests are listed in Tables 6, 7 and 8.

Table 6 – P-values for comparison of mean composite NTCP values

Test	P-value
Prostate CTV vs. SIB CTV	0.343
Prostate CTV Sum vs. SIB CTV Sum	0.128
SIB CTV vs. SIB CTV Sum	0.736
Prostate CTV vs. Prostate CTV Sum	0.832

Table 7 – P-values for comparison of mean composite TCP with α/β = 1.5

Test	P-value
Prostate CTV vs. SIB CTV	< 0.001
Prostate CTV Sum vs. SIB CTV Sum	< 0.001
SIB CTV vs. SIB CTV Sum	0.821
Prostate CTV vs. Prostate CTV Sum	0.305

Table 8 – P-values for comparison of mean composite TCP with α/β = 3.0

Test	P-value
Prostate CTV vs. SIB CTV	< 0.001
Prostate CTV Sum vs. SIB CTV Sum	< 0.001
SIB CTV vs. SIB CTV Sum	0.829
Prostate CTV vs. Prostate CTV Sum	0.270

CHAPTER 5. DISCUSSION

5.1 Summary of Results

The results of the TCP and NTCP calculations may be analyzed in several different ways to assess the clinical superiority of DIL-SIB plans using IMPT. First, the direct benefits of the SIB plans may be evaluated by comparing their TCP and NTCP values with the conventional plans, considering both the nominal and composite forms. It may be observed that the SIB plans have much higher mean composite TCP values than the conventional plans, both nominal and composite. The small p-values of the tests comparing TCP for Prostate CTV vs. SIB CTV and Prostate CTV Sum vs. SIB CTV Sum show that these differences are highly significant. This observation is true when considering the mean composite TCP for both values of α/β. Closer examination of the individual TCP values show a large increase for the DIL in the SIB plans, with a smaller increase for the CTV. This is the expected result, as the focal boost to the DIL volume will increase its TCP while also delivering additional residual dose to the CTV. Comparison of the mean composite NTCP shows a small increase in the nominal and composite SIB plans from the conventional. This same observation may be made of the individual NTCP values for each OAR. A marginal increase in the probability of normal tissue toxicities is also expected in the SIB plans due to the higher doses associated with the focal spot. This increase is not significant based on the tests comparing the NTCP of Prostate CTV vs. SIB CTV and Prostate CTV Sum vs. SIB CTV Sum. These initial observations are promising, as they support the ability of the SIB plans to achieve better tumor control with minimal increase in the occurrence of normal tissue toxicities. The higher P+ values of the SIB plans with

either α/β ratio also convey these findings. The second and more pertinent question that may be addressed from the data is whether the dosimetric variation in the composite SIB plans leads to a significant degradation of tumor control or an increase in the likelihood of normal tissue damage. This question may be assessed through comparison of the results in a different way, with the nominal SIB and conventional plans contrasted against their composite forms. The mean composite TCP value for the composite conventional plan shows a small decrease from the nominal plan. This is yet another expected result, as the dose variation reflected in the composite plan can lead to a lack of target coverage. Surprisingly, a small increase may be seen in the mean composite TCP of the SIB plans due to the variation. This could be the product of a higher dose delivered to the CTV through variation in the focal spot position, while still maintaining sufficient DIL coverage. These observations are also consistent for both α/β ratios and the individual TCPs of the DIL and CTV. The p-values for SIB CTV vs. SIB CTV Sum and Prostate CTV vs. Prostate CTV Sum show that neither the decrease in mean composite TCP for the conventional plans or the increase for the SIB plans is significant. Lastly, examination of mean composite NTCP reveals a small increase in the SIB plans from the dosimetric variation. This is expected due to the likelihood of a higher dose to normal tissues from focal spot deviation. The same slight increase is seen in the mean NTCP values for each OAR. When comparing the NTCP values for the nominal and composite conventional plans, an unexpected decrease in NTCP may be seen. The explanation for a lower NTCP when considering dosimetric variation is not immediately clear. The difference could be the result of a methodological error such as the choice of OARs. Examination of the p-values

for comparison of SIB CTV vs. SIB CTV Sum and Prostate CTV vs. Prostate CTV Sum again reveal minimal significance of the observed differences in NTCP.

5.2 Limitations

Despite the compelling observations made from the results, possible shortcomings of the methodology must be noted to contextualize any conclusions. One limitation lies in the inherent uncertainties associated with the biological modelling. While TCP and NTCP are useful metrics for the comparison or optimization of plans with different dose distributions and fractionation schedules, they are not always accurate predictors of clinical outcomes. The choices of models, parameters, OARs, and endpoints all affect the results of TCP and NTCP calculations. Different models using parameters obtained with varying methods and patient populations will seldom yield identical results. The practical limitation on the number of OARs and endpoints that are considered for NTCP calculations can also alter the outcome. It is possible that dosimetric variation in the SIB plans may lead to toxicities in normal tissues that were not considered, or different endpoints in the tissues that were. Another limitation of the methodology is in the assumption that any dosimetric variation from patient anatomy changes occurring during the first week are representative of the entire treatment course. Since most of the patients only received the several daily CBCT scans during the first treatment week, this was the only data representing any anatomic changes that was available for this study. It is possible that more significant changes could occur over a longer period of the treatment, leading to larger dose shifts and further normal tissue damage or loss of target coverage. A compelling argument supporting the viability of the methodology may be made by considering the TCP and NTCP calculations for individual patients. As mentioned in the methods section, several of the patients received

additional CBCT scans over longer periods of time. It may be observed that the TCP and NTCP values for these specific patients are not significantly different from the averages. These individual values are also consistent with the conclusions of the various hypothesis tests. Therefore, it is probable that no significant variations in TCP or NTCP would occur if the anatomy changes from a longer period of the treatment were represented in the analysis. A final limitation in the methodology that should be discussed is the possible influence of range uncertainties on the results. As outlined in the background section, the inaccurate calculation of proton stopping powers from CT scans can lead to additional variation in the delivered dose distribution. The effects of possible uncertainties in proton ranges may be simulated in most treatment planning systems but were not incorporated into the plans considered by this study. The plans were, however, optimized based on the robustness objectives specified in the methods section. This optimization and the additional margin added to the target should significantly reduce the susceptibility of the plans to any range variations. Other studies have also shown that setup and range uncertainties only have a small effect on TCP and NTCP in IMPT plans, even without robust optimization (32). Although it may be unlikely that range variations would have significantly altered the TCP and NTCP calculations for the conventional plans, it is possible that the focal boost in the SIB plans could worsen the effects. Further investigation into the effects of range uncertainties on TCP and NTCP in IMPT DIL-SIB would therefore be useful. A potential solution to the problem of both range and anatomic variations is adaptive radiotherapy, in which treatment plans are optimized between fractions to account for any dosimetric changes. This continuous updating of plans can reduce the extra margins required to account for variations, and ultimately improve therapeutic ratios (33).

CONCLUSIONS

Two main conclusions may be drawn from the analysis that support the clinical superiority of DIL-SIB in IMPT. One is that DIL-SIB almost certainly increases the tumor control of both the DIL and CTV, with no major changes in the standard possibilities for normal tissue toxicities. The second conclusion is that DIL-SIB plans are not any more susceptible to the biological effects of interfractional dosimetric variation than conventional plans. These conclusions therefore suggest that DIL-SIB is a reasonably safe and effective way to achieve better prostate tumor control with IMPT than uniform irradiation plans. The results of this study are a promising piece of theoretical evidence supporting the clinical use of DIL-SIB in IMPT. To confirm the actual benefits and safety of these plans as suggested by the TCP and NTCP calculations, studies of clinical outcomes must be performed. These studies would have a similar structure as those that have supported photon DIL-SIB, investigating endpoints such as disease-free patient survival and complications. Further demonstration that DIL-SIB using IMPT offers improved outcomes when compared with traditional IMPT or other modalities would support the overall use of proton therapy in the treatment of prostate cancer.

REFERENCES

1. American Cancer Society. Cancer Facts and Figures 2020.

2. Wisenbaugh ES, Andrews PE, Ferrigni RG, et al. Proton beam therapy for localized prostate cancer 101: basics, controversies, and facts. *Rev Urol*. 2014;16(2):67-75.

3. Royce TJ, Efstathiou JA. Proton therapy for prostate cancer: A review of the rationale, evidence, and current state. *Urol Oncol*. 2019;37(9):628-636.

4. Khan FM, Gibbons JP. *The Physics of Radiation Therapy*. 5th Edition. Philadelphia: Lippincott Williams & Wilkins; 2014. 524-540 p.

5. Trofimov A, Nguyen PL, Efstathiou JA, et al. Interfractional variations in the setup of pelvic bony anatomy and soft tissue, and their implications on the delivery of proton therapy for localized prostate cancer. *Int J Radiat Oncol Biol Phys*. 2011;80(3):928-37.

6. Lin L, Vargas C, Hsi W, et al. Dosimetric uncertainty in prostate cancer proton radiotherapy. *Med Phys*. 2008;35(11):4800-7.

7. Lee J, Carver E, Feldman A, Pantelic MV, Elshaikh M, Wen N. Volumetric and Voxel-Wise Analysis of Dominant Intraprostatic Lesions on Multiparametric MRI. Front Oncol. 2019;9:616.

8. Wang T, Press RH, Giles M, et al. Multiparametric MRI-guided dose boost to dominant intraprostatic lesions in CT-based High-dose-rate prostate brachytherapy. *Br J Radiol*. 2019;92(1097)

9. Orlandi E, Palazzi M, Pignoli E, et al. Radiobiological basis and clinical results of the simultaneous integrated boost (SIB) in intensity modulated radiotherapy (IMRT) for head and neck cancer: A review. *Crit Rev Oncol Hematol*. 2010;73(2):111-25.

10. Monninkhof EM, van Loon JWL, van Vulpen M, et al. Standard whole prostate gland radiotherapy with and without lesion boost in prostate cancer: Toxicity in the FLAME randomized controlled trial. *Radiother Oncol*. 2018;127(1):74-80.

11. Kerkmeijer LGW, Groen VH, Pos FJ, et al. Focal Boost to the Intraprostatic Tumor in External Beam Radiotherapy for Patients With Localized Prostate Cancer: Results From the FLAME Randomized Phase III Trial. *J Clin Oncol*. 2021;39(7):787-796.

12. Andrzejewski P, Kuess P, Knäusl B, et al. Feasibility of dominant intraprostatic lesion boosting using advanced photon-, proton- or brachytherapy. *Radiother Oncol*. 2015;117(3):509-14.

13. Wang T, Zhou J, Tian S, et al. A planning study of focal dose escalations to multiparametric MRI-defined dominant intraprostatic lesions in prostate proton radiation therapy. *Br J Radiol*. 2020;93(1107)

14. Unkelbach J, Paganetti H. Robust Proton Treatment Planning: Physical and Biological Optimization. *Semin Radiat Oncol*. 2018 Apr;28(2):88-96.

15. Fiorino C, Valdagni R, Rancati T, et al. Dose-volume effects for normal tissues in external radiotherapy: pelvis. *Radiother Oncol*. 2009;93(2):153-67.

16. Michalski JM, Gay H, Jackson A, Tucker SL, Deasy JO. Radiation dose-volume effects in radiation-induced rectal injury. *Int J Radiat Oncol Biol Phys*. 2010;76(3 Suppl):S123-9.

17. Viswanathan AN, Yorke ED, Marks LB, et al. Radiation dose-volume effects of the urinary bladder. *Int J Radiat Oncol Biol Phys*. 2010;76(3 Suppl):S116-22.

18. Panettieri V, Rancati T, Onjukka E, et al. External Validation of a Predictive Model of Urethral Strictures for Prostate Patients Treated With HDR Brachytherapy Boost. *Front Oncol*. 2020;10:910.

19. Hall EJ, Giaccia AJ. *Radiobiology for the Radiologist*. 7th Edition. Philadelphia: Lippincott Williams & Wilkins; 2012. 327-354 p.

20. Tommasino F, Nahum A, Cella L. Increasing the power of tumour control and normal tissue complication probability modelling in radiotherapy: recent trends and current issues. *Translational Cancer Research.* 2017;6(S5): S807-S821.

21. Mesbahi A, Oladghaffari M. An Overview on the Clinical Application of Radiobiological Modeling in Radiation Therapy of Cancer. *International Journal of Radiology & Radiation Therapy*. 2017;2(1).

22. Lind BK, Mavroidis P, Hyödynmaa S, et al. Optimization of the dose level for a given treatment plan to maximize the complication-free tumor cure. *Acta Oncol*. 1999;38(6):787-98.

23. RaySearch Laboratories. RayStation 9A Reference Manuel. 2020.

24. Azzeroni R, Maggio A, Fiorino C, et al. Biological optimization of simultaneous boost on intra-prostatic lesions (DILs): sensitivity to TCP parameters. *Phys Med*. 2013;29(6):592-8.

25. Sachpazidis I, Mavroidis P, Zamboglou C, et al. Prostate cancer tumour control probability modelling for external beam radiotherapy based on multi-parametric MRI-GTV definition. *Radiat Oncol*. 2020;15(242).

26. Vogelius IR, Bentzen SM. Meta-analysis of the alpha/beta ratio for prostate cancer in the presence of an overall time factor: bad news, good news, or no news? *Int J Radiat Oncol Biol Phys*. 2013;85(1):89-94.

27. Källman P, Agren A, Brahme A. Tumour and normal tissue responses to fractionated non-uniform dose delivery. *Int J Radiat Biol*. 1992;62(2):249-62.

28. Lyman JT. Complication probability as assessed from dose-volume histograms. *Radiat Res Suppl*. 1985;8:S13-9.

29. Takam R, Bezak E, Yeoh EE. Assessment of normal tissue complications following prostate cancer irradiation: comparison of radiation treatment modalities using NTCP models. *Med Phys*. 2010;37(9):5126-37.

30. Ågren Cronqvist AK. *Quantification of the response of heterogeneous tumours and organized normal tissues to fractionated radiotherapy*. [PhD Thesis]. Stockholm: Stockholm University; 1995.

31. Zhou J, Tian S, Patel SA, et al. Online Prediction of Dosimetric Changes in Dominant Intraprostatic Lesion Simultaneous Boost Using Intensity Modulated Proton Therapy. *Int J Radiat Oncol Biol Phys*. 2020;108(3 Suppl):S170-171.

32. Hamming-Vrieze O, Depauw N, Craft DL, et al. Impact of setup and range uncertainties on TCP and NTCP following VMAT or IMPT of oropharyngeal cancer patients. *Phys Med Biol.* 2019;64(9):095001.

33. Ghilezan M, Yan D, Martinez A. Adaptive radiation therapy for prostate cancer. *Semin Radiat Oncol.* 2010;20(2):130-137.